Journal of the Korean Physical Society, Vol. 46, No. 5, May 2005, pp. 1170∼1173

Fabrication of Isolated Magnetic Nanostructures by Using Nanoporous Anodic Alumina Films on Si

S. G. Lee, S. W. Shin and J. Lee*
Institute of Physics and Applied Physics, Yonsei University, Seoul 120-749

J. H. Lee
Department of Materials Science and Engineering, Korea University, Seoul 136-701

T. G. Kim and J. H. Song
Advanced Analysis Center, Korea Institute of Science and Technology, Seoul 130-650

(Received 3 February 2005, in final form 9 March 2005)

Arrays of magnetic Ni nanostructures have been fabricated on a Si substrate by using a nanoporous alumina film as a mask during the deposition. The nanostructures have a truncated cone shape, and the lateral sizes are comparable to the heights. While a continuous film shows well-defined in-plane magnetization, the nanostructure has a perpendicular component of the magnetization at remanence. The hysteretic behavior of the nanostructures is dominated by the demagnetizing field instead of by interaction among the structures.

PACS numbers: 75.30.Gw, 73.61.Tm, 75.60.Ej
Keywords: Magnetic nanostructure, Magnetic anisotropy, Demagnetizing field, AAO

I. INTRODUCTION

Arrays of magnetic nanostructures have been studied to extend the superparamagnetic limit within a few years, thereby increasing the storage density by one order of magnitude [1]. The standard approach for fabricating nanostructures is to combine thin-film growth techniques with sub-micron lithography. However, this method has intrinsic drawbacks; it has low throughput and high equipment cost, and is a time-consuming procedure. Various methods have been applied to produce nanoparticles, such as chemical process [2, 3], and to produce arrays of nanostructures, such as self-organization phenomena [4–6], including nanoporous anodic alumina [7–9]. Aluminum is known to form self-organized nanopore arrays during the anodization process. The extreme high aspect ratio (ratio of length to diameter) makes anodic alumina an ideal template material for fabricating nanowires [10–14]. However, careful handling of thin nanoporous alumina (less than 500 nm) obtained by anodizing Al foil is required when it is used as a mask in fabricating nanostructures on a foreign substrate [15].

Recently, there have been reports of the anodization of an Al film deposited on a substrate [16–19]. This allows the direct deposition of nanostructures on any substrate with high reproducibility and uniformity [17], which is desirable for device applications. Moreover, the aspect ratio can be manipulated easily. Therefore, a nanoporous alumina film on a substrate is better suited to applications than the nanoporous alumina foil. Also, several interesting results have already been reported, such as pattern transfer to the substrate [16,17], fabrication of metal [17], and fabrication of metal oxide [18]. The ordering of the nanoarray can be improved by using prepattering [17–19].

In this paper, we report the fabrication of an array of Ni nanostructures on Si substrate. Nanoporous alumina film was used as a mask for local deposition of Ni during evaporation. The isolated Ni nanostructures were fabricated by removing porous alumina material after deposition. The magnetic properties of the Ni nanostructures are compared with those of a continuous Ni film with the same thickness.

II. EXPERIMENT

An 800 nm thick Al film on Si with natural oxide prepared by using electron beam evaporation was anodized in two steps [7,8]. The first anodization was carried out in a 0.3 M oxalic acid ($C_2H_2O_4$) at 140 V for 430 s. The temperature was maintained at 3 °C during the anodization process. After the first anodization, the produced alumina layer was removed by using a mixed solution of

*E-mail: jl10017@phya.yonsei.ac.kr; Fax: +82-2-392-1592

6 % phosphoric acid (H_3PO_4) and 6 % chromium trioxide in water (CrO_3) for 30 min at 53 °C in order to adjust the aspect ratio of the nanopores. Next, the second anodization was carried out for 80 sec under the same anodization conditions as the first one. A 0.2-M phosphoric acid was used to increase the pore diameter.

A 70-nm thick Ni film was thermally deposited onto nanoporous alumina on Si in vacuum with a deposition rate of 0.03 nm/sec. The pressure was 1×10^{-8} Torr during the evaporation. After Ni deposition, the alumina was removed by dipping into 5-M NaOH at 50 °C and 0.2 M phosphoric-acid solutions at 53 °C sequentially.

The Ni nanostructures was monitored by using a field emission scanning electron microscope (FESEM: JEOL 6500F). The macroscopic hysteresis loops of the nanostructure and the continuous 70-nm-thick Ni film were measured by using the magneto-optic Kerr effect (MOKE) in the polar and the longitudinal configurations.

III. RESULTS AND DISCUSSION

Fig. 1 shows the SEM images of the nanoporous alumina mask after the pore widening process. The diameter of a pore is around 60 – 90 nm, and the wall thickness between pores is around 15 – 30 nm. The ordering of the pores is poor because the Al film is known to have much smaller grain size than polycrystalline bulk Al [19]. The inset shows the SEM image of the sideview. The pore height is 170 nm, which helps the deposition inside nanopores. The pores are straight down to the Si substrate. Usually, the alumina barrier layer is separated from the Si at the end of the anodization, thus forming voids between the barrier and the Si [16]. The subsequent widening process widens the pore diameter and removes voids by removing the alumina barrier layer as well, which makes straight-through holes.

The SEM images after Ni evaporation are shown in Fig. 2(a). The pore diameter decreases and the wall thickness increases because Ni is deposited on the wall during evaporation. The existence of pores implies that

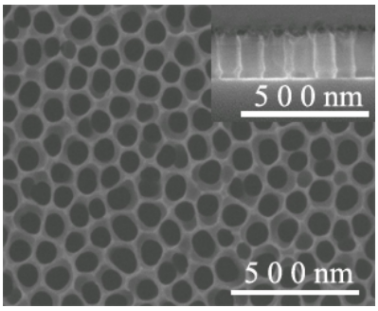

Fig. 1. SEM image of the topview of a nanoporous alumina film on Si. The inset shows the SEM image of the sideview.

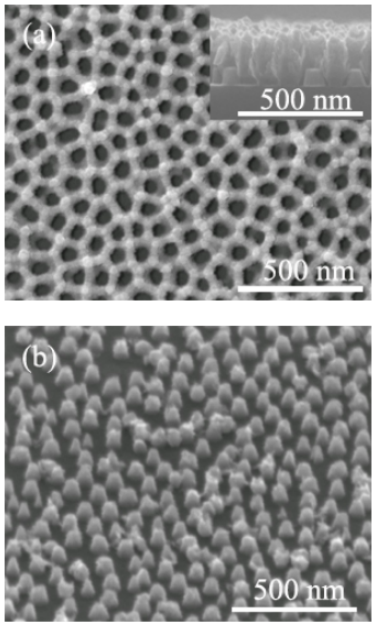

Fig. 2. 2 (a) SEM image of the topview after Ni evaporation. The inset shows the SEM image of the sideview. The Ni nanostructures with truncated cone-shapes are clearly visible in the side-view. (b) Three-dimensional view of the isolated Ni nanostructures after removing alumina mask.

the Ni is also deposited at the bottom of the pore. This is supported by the side-view SEM image as in the inset, which shows truncated cone-shaped Ni nanostructures inside pores and very thick walls separating nanostructures. The nanostructures are 70 nm high with a comparable lateral size. The ratio of the lateral size at the bottom to the size at the top is close to 2. The size of nanostructure at the bottom is determined by the initial pore size. As evaporation proceeds, the material deposited on the wall increases, which gradually decreases the diameter of the nanostructure as the nanostructure becomes thicker. Fig. 2(b) shows the three-dimensional SEM image of the isolated Ni nanostructures on Si after removing the alumina chemically. The density of the Ni nanostructure is $\sim 1 \times 10^{10}/\mathrm{cm}^2$. The lateral size and the arrangement of the nanostructures are in accord with the nanoporous alumina mask. The truncated cone-shape is maintained after chemical etching.

The magnetic properties of the Ni nanostructures on a Si substrate are compared with those of a Ni film with the same thickness on the Si substrate. Fig. 3(a) shows the hysteresis loops with the magnetic field parallel to the Si surface. The hysteresis loop of the continuous film shows a well-defined switching field ($\sim$ 370 Oe) and a saturation field ($\sim$ 950 Oe). The magnetization at remanence is $\sim$ 45 % of the saturation magnetization (M_S), which is close to the value of noninteracting particles with a randomly oriented easy axis [20]. The measurements performed by varying the magnetic field directions in the plane confirmed that the magnetization of

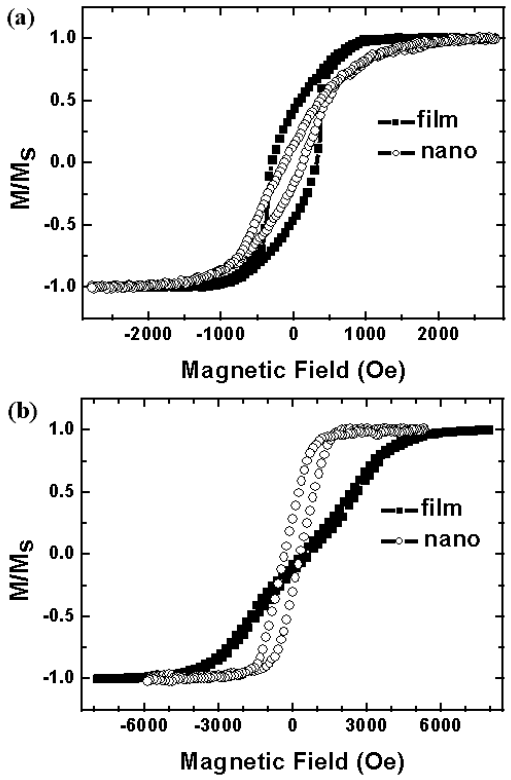

Fig. 3. Hysteresis loops of a continuous film and isolated nanostructures measured with the fields (a) parallel and (b) perpendicular to the surface of the Si substrate.

the continuous film is isotropic in the plane. Therefore, the magnetization points into arbitrary directions at remanence, which decreases the remanent magnetization. The hysteresis loop of the Ni nanostructure shows a different behavior. It has neither a well-defined switching field nor a saturation field. The magnetization at remanence ($\sim 0.14M_S$) and the coercive field are smaller than those of the continuous film. More dramatic changes in the hysteretic behavior are observed when the magnetic field is applied perpendicular to the Si surface as shown in Fig. 3(b). The saturation field of the continuous film is ~ 6 kOe, and the magnetization at remanence is negligible, which means that the magnetic property is determined by the demagnetizing field. The saturation field and the magnetization at remanence of the nanostructures are ~ 2 kOe and $\sim 0.3M_S$, respectively, which indicate that their magnetic properties are so strongly influenced by their shape that some of the nanostructures have a perpendicular component of the magnetization. The magnetization does not lie in the plane any more. The coercivity of the nanostructure is ~ 300 Oe.

The fact that the Ni continuous film is magnetically isotropic in the plane means that it possesses a polycrystalline structure. It is conceivable that the demagnetizing field will affect the hysterectic behavior of the nanostructure with the assumption that the nanostructure has the same polycrystalline structure as that of the continuous film. The demagnetizing factor in the direction of the cone axis can be determined from the slope of the hysteresis loop measured with the field perpendicular to the Si surface [21]. The saturation magnetization of the nanostructure is assumed to be equivalent to the bulk value, $M_s = 484$ emu/cm^3. The determined demagnetizing factor is 0.175 ± 0.0047, which is very close to the value of a cylinder with a aspect ratio of 1.5 [22]. It is well known that the demagnetizing factor is sensitive to the actual shape of the structure. However, this value of the demagnetizing factor can be expected because the shape of the nanostructure is similar to that of a cylinder with an aspect ratio of 1.5. This indicates that the demagnetizing field dominates the hysterectic behavior of these nanostructures. This is clearly different from the behavior of magnetic nanowires, where the interaction among the magnetic nanowires, in addition to the demagnetizing field, plays an important role in the hysterectic behavior [11–13].

IV. CONCLUSION

In summary, magnetic nanostructures were prepared on a Si substrate by evaporating Ni in vacuum. The nanoporous alumina prepared by anodizing Al film on a Si substrate was used as a mask for nanoscale deposition during evaporation. The magnetization of the nanostructure at remanence was not confined to the plane while the continuous film with the same thickness had an easy magnetization direction in the plane. It is concluded that the hysterectic behavior along the cone axis is strongly affected by the demagnetizing field rather than by the interaction among nanostructures.

ACKNOWLEDGMENTS

This work was supported by grant No. R01-2004-000-10715-0 from the Basic Research Program of the Korea Science & Engineering Foundation, Korea Research Foundation Grant (KRF-2004-015-C00170), and by the R & D Program for NT-IT Fusion Strategy of Advanced Technologies.

REFERENCES

[1] D. Weller and A. Moser, IEEE Trans. Magn. **35**, 4423 (1999).
[2] I. Rhee and C. Kim, J. Korean Phys. Soc. **42**, 175 (2003).
[3] G. H. Lee, S. H. Huh, S. J. Oh, B. Kim and J. Park, J. Korean Phys. Soc. **44**, 1499 (2004).
[4] G. M. Whitesides, J. P. Mathias and C. T. Seto, Science **254**, 1312 (1991).

[5] M. Park, C. Harrison, P. M. Chaikin, R. A. Register and D. H. Adamson, Science **276**, 1401 (1997).
[6] J. Y. Yang, K. S. Yoon, Y. H. Do, J. H. Koo, C. O. Kim, J. P. Hong, S. O. Sohn, S. K. Min and H. J. Kim, J. Korean Phys. Soc. **45**, 124 (2004).
[7] H. Masuda and K. Fukuda, Science **268**, 1466 (1995).
[8] H. Masuda, H. Yamada, M. Satoh, H. Asoh, M. Nakao and T. Tamamura, Appl. Phys. Lett. **71**, 2770, (1997).
[9] S. K. Thamida and H. C. Chang, Chaos, **12**, 240 (2002).
[10] J. S. Suh and J. S. Lee, Appl. Phys. Lett. **75**, 2047 (1999).
[11] J. M. García, A. Asenjo, J. Velázquez, D. García, M. Vázquez, P. Aranda and E. Ruiz-Hitzky, J. Appl. Phys. **85**, 5480 (1999).
[12] H. Cao, C. Tie, Z. Xu, J. Hong and H. Sang, Appl. Phys. Lett. **78**, 1592 (2001).
[13] K. Nielsch, R. B. Wehrspohn, J. Barthel, J. Kirschner and U. Gosele, Appl. Phys. Lett. **79**, 1360 (2001).
[14] A. J. Yin, J. Li, W. Jian, A. J. Bennett and J. M. Xu, Appl. Phys. Lett. **79**, 1039 (2001).
[15] J. Liang, H. Chik, A. Yin and J. Xu, J. Appl. Phys. **91**, 2544 (2002).
[16] D. Crouse, Y-H. Lo, A. E. Miller and M. Crouse, Appl. Phys. Lett. **76**, 49 (2000).
[17] H. Masuda, K. Yasui, Y. Sakamoto, M. Nakao, T. Tamamura and K. Nishio, Jpn. J. Appl. Phys. **40**, L1267 (2001).
[18] P. L. Chen, C. T. Kuo, T. G. Tsai, B. W. Wu, C. C. Hsu and F. M. Pan, Appl. Phys. Lett. **82**, 2796 (2003).
[19] Z. Sun and H. K. Kim, Appl. Phys. Lett. **81**, 3458 (2002).
[20] E. C. Stoner and E. P. Wohlfarth, Phil. Trans. Roy. Soc. A **240**, 599 (1948).
[21] R. C. O'Handley, *Modern Magnetic Materials Principle and Applications*, (Wiley & Sons, New York, 2000), p. 31.
[22] B. D. Cullity, *Introduction to Magnetic Materials*, (Addison-Wesley, Massachusetts, 1972), p. 58.